

## Nondestructive identification of isotopes using nuclear resonance fluorescence

Toshiyuki Shizuma, Takehito Hayakawa, Ryoichi Hajima, Nobuhiro Kikuzawa, Hideaki Ohgaki et al.

Citation: *Rev. Sci. Instrum.* **83**, 015103 (2012); doi: 10.1063/1.3673002

View online: <http://dx.doi.org/10.1063/1.3673002>

View Table of Contents: <http://rsi.aip.org/resource/1/RSINAK/v83/i1>

Published by the [American Institute of Physics](#).

---

### Related Articles

A new borehole wire extensometer with high accuracy and stability for observation of local geodynamic processes

*Rev. Sci. Instrum.* **83**, 015109 (2012)

Theoretical investigation of the water/corundum (0001) interface

*J. Chem. Phys.* **130**, 064702 (2009)

Static and flowing regions in granular collapses down channels: Insights from a sedimenting shallow water model

*Phys. Fluids* **19**, 106601 (2007)

Self-organization of hydrophobic soil and granular surfaces

*Appl. Phys. Lett.* **90**, 054110 (2007)

Selection of the ripple length on a granular bed sheared by a liquid flow

*Phys. Fluids* **18**, 121508 (2006)

---

### Additional information on *Rev. Sci. Instrum.*


Journal Homepage: <http://rsi.aip.org>

Journal Information: [http://rsi.aip.org/about/about\\_the\\_journal](http://rsi.aip.org/about/about_the_journal)


Top downloads: [http://rsi.aip.org/features/most\\_downloaded](http://rsi.aip.org/features/most_downloaded)

Information for Authors: <http://rsi.aip.org/authors>

## ADVERTISEMENT



**Does your research require low temperatures? Contact Janis today.**  
**Our engineers will assist you in choosing the best system for your application.**



**10 mK to 800 K**  
**Cryocoolers**  
**Dilution Refrigerator Systems**  
**Micro-manipulated Probe Stations**

**LHe/LN<sub>2</sub> Cryostats**  
**Magnet Systems**

**sales@janis.com    www.janis.com**  
**Click to view our product web page.**

# Nondestructive identification of isotopes using nuclear resonance fluorescence

Toshiyuki Shizuma,<sup>1,a)</sup> Takehito Hayakawa,<sup>1</sup> Ryoichi Hajima,<sup>1</sup> Nobuhiro Kikuzawa,<sup>2</sup> Hideaki Ohgaki,<sup>3</sup> and Hiroyuki Toyokawa<sup>4</sup>

<sup>1</sup>Quantum Beam Science Directorate, Japan Atomic Energy Agency, Tokai, Ibaraki 319-1195, Japan

<sup>2</sup>J-PARC Center, Japan Atomic Energy Agency, Tokai, Ibaraki 319-1195, Japan

<sup>3</sup>Institute of Advanced Energy, Kyoto University, Uji, Kyoto 611-0011, Japan

<sup>4</sup>National Institute of Advanced Industrial Science and Technology, Tsukuba, Ibaraki 305-8568, Japan

(Received 16 September 2011; accepted 5 December 2011; published online 5 January 2012)

Nondestructive identification of heavy isotopes concealed in a thick iron box has been demonstrated by using nuclear resonance fluorescence. A quasi-monochromatic photon beam produced by the collision of laser quanta with high energy electrons was used for resonant excitation of nuclear levels in  $^{206}\text{Pb}$  and  $^{208}\text{Pb}$ . By measuring the resonant  $\gamma$  rays emitted from  $^{206}\text{Pb}$  and  $^{208}\text{Pb}$ , each of these isotopes were clearly identified. The ratio of the effective thickness, i.e., concentration distribution, of these isotopes was deduced from the relative intensities of the measured nuclear resonance fluorescence strengths. © 2012 American Institute of Physics. [doi:10.1063/1.3673002]

## I. INTRODUCTION

Nondestructive assay (NDA) of fissile materials is a key subject in international nuclear security and safeguard perspectives.<sup>1</sup> Particularly, the isotope-specific identification is required for the quantification of nuclear materials in spent fuel assemblies.<sup>2,3</sup> Although the conventional NDA technique using x-ray fluorescence can be used for identification of elements, it cannot be applied for the discrimination of isotopes in the same element. For nuclear safeguard problems, it is of increasing importance to quantify isotopic concentration distribution of nuclear materials, e.g.,  $^{235}\text{U}$  and  $^{238}\text{U}$ . Nuclear resonance fluorescence (NRF) is one method which can be used to determine the isotopic composition of sample materials in a nondestructive way.<sup>4-6</sup> The NRF, primarily used for nuclear structure investigation,<sup>7,8</sup> is a process of resonant excitation of nuclear levels by absorption of photons and subsequent de-excitation to lower-lying levels by  $\gamma$ -ray emission. Since each nucleus has characteristic resonant energies, the detection of resonant  $\gamma$  rays provides a unique fingerprint identifying that nucleus. High-energy  $\gamma$  rays used for resonant excitation have high penetrability of materials. Thus, the NRF technique can be applied for elemental and isotopic characterization of thick materials consisted of heavy metals. In the present study, we demonstrate isotope-specific identification of lead isotopes,  $^{206}\text{Pb}$  and  $^{208}\text{Pb}$ , concealed in a thick iron box by using the NRF method with a quasi-monochromatic photon beam.

## II. EXPERIMENTAL PROCEDURE

A schematic view of the present detection method using NRF is depicted in Fig. 1. The lead nuclei of  $^{206}\text{Pb}$  and  $^{208}\text{Pb}$  have several  $1^-$  levels which can be resonantly excited by photo-absorption. The energy of an incident photon beam

is matched to the resonant energy of  $^{206}\text{Pb}$  or  $^{208}\text{Pb}$  in order to excite these nuclei. By detecting the de-exciting  $\gamma$  rays to the ground state, each of these nuclei can be identified.

The NRF measurements have been carried out at the Tsukuba Electron Ring for Acceleration and Storage (TERAS) facility of the National Institute of Advanced Industrial Science and Technology (AIST). The laser Compton scattering (LCS) photon beam line is depicted in Fig. 2. A quasi-monochromatic, linearly polarized photon beam was generated by the inverse Compton scattering of laser light with high-energy electrons.<sup>9</sup> A Nd:YVO<sub>4</sub> Q-switch laser at wavelength of 1064 nm operated at a frequency of 20 kHz was used. The electron energies were selected at 563 and 584 MeV to produce LCS photons with the maximum energy of  $E_{\gamma}^{\text{max}} = 5.6$  and 6.0 MeV, respectively. A 20 cm lead collimator with 2 mm aperture was placed between the collision point and the target to form a quasi-monochromatic photon beam with a typical energy spreading width of  $\Delta E_{\gamma}/E_{\gamma} \approx 10\%$  in full width at half maximum (FWHM).

The target and detector setup is also shown in Fig. 2. The NRF  $\gamma$  rays from the target were detected by a high-purity (HP) Ge detector with a relative efficiency of 140%, placed at a scattering angle of  $\theta = 90^\circ$  with respect to the beam direction. The energy resolution of the Ge detector was approximately 6 keV in FWHM at  $E_{\gamma} \sim 7$  MeV. Events correlated with laser pulses within 1  $\mu\text{s}$  were collected to reduce background counts originated from the continuous bremsstrahlung photons from high energy electrons circulating in the storage ring. The  $\gamma$ -ray energies were calibrated using natural background lines (1460.8 and 2614.5 keV).

Figure 3 shows an energy spectrum of the incident LCS photons measured by an HP-Ge detector with a relative efficiency of 120%. A Monte Carlo simulation was performed with the EGS4 code<sup>10</sup> to analyze the response of the HP-Ge detector. The energy distribution of incident LCS photons was extracted by unfolding the simulated spectrum which repro-

<sup>a)</sup>Electronic mail: shizuma.toshiyuki@jaea.go.jp.

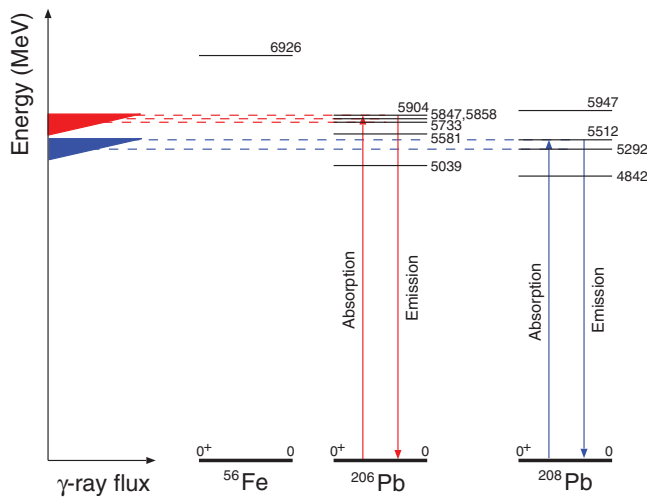


FIG. 1. (Color online) Selected  $1^-$  resonant levels with  $\Gamma_0 > 1$  eV below  $E_x = 6$  MeV in  $^{206}\text{Pb}$  and  $^{208}\text{Pb}$ . No corresponding level exists in  $^{56}\text{Fe}$ , the main component of the iron box. When the energy of the incident photon beam overlaps with the resonant energies of  $^{206}\text{Pb}$  ( $^{208}\text{Pb}$ ) as shown by the red (blue) broken lines, the incident photons are absorbed by the  $^{206}\text{Pb}$  ( $^{208}\text{Pb}$ ) nucleus. The emitted  $\gamma$  rays at the resonant energies of  $^{206}\text{Pb}$  (5616, 5847, and 5904 keV) and of  $^{208}\text{Pb}$  (5292 and 5512 keV) are detected by an HP-Ge detector.  $^{56}\text{Fe}$  is off-resonant at these energies of the incident  $\gamma$ -ray beams.

duces the observed energy distribution. The unfolded spectrum was used to deduce the intensities of the incident photon beam at the energies of interest.

The number of LCS photons was monitored during the experiment using a large volume ( $8'' \times 12''$ ) NaI scintillator placed behind the targets. The pulse height of the spectrum is proportional to the number of LCS photons per beam pulse. Thus, the intensity of the incident photon beam can be obtained by multiplying the average photon number per beam pulse and the frequency of the beam pulse.<sup>11</sup> The average beam intensity during the measurement was  $\approx 1.5 \times 10^5$  photons/s.

The target concealed in an iron box consists of two pieces of natural lead blocks and an enriched  $^{206}\text{Pb}$  sample as shown in Fig. 4. Metallic granules of  $^{206}\text{Pb}$  were packed in a plastic cylinder. Both the front and the back side thickness of the iron box is 15 mm. The sizes of the natural lead blocks and the  $^{206}\text{Pb}$  cylinder are  $15 \times 15 \times 10$  mm<sup>3</sup> and 15-mm length with 7-mm diameter, respectively. The natural lead contains  $^{208}\text{Pb}$  with isotopic abundance of 52.4%. The enrichment and density of the  $^{206}\text{Pb}$  sample is 99.3% and 6.9 g/cm<sup>3</sup>. The effective thickness of  $^{208}\text{Pb}$  and  $^{206}\text{Pb}$  is 8.9 and 10 g/cm<sup>2</sup>, respec-

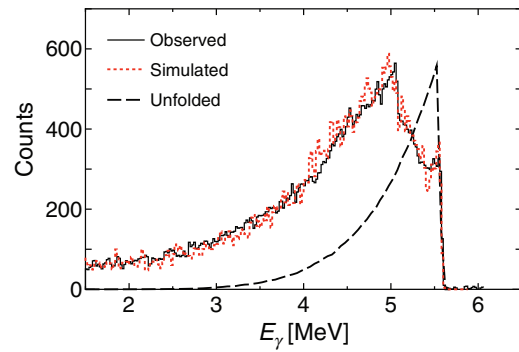


FIG. 3. (Color online) An observed spectrum of the incident LCS photons measured with an HP-Ge detector (solid line). The original LCS photons shown in the dashed line was obtained by unfolding the simulated energy distribution (dotted line).

tively. The target was placed on an elevation stage to measure the NRF events as a function of the vertical position, i.e., the  $z$ -direction. The iron-concealed  $^{208}\text{Pb}$  ( $^{206}\text{Pb}$ ) target was irradiated with the LCS photon beam at  $E_\gamma^{\text{max}} = 5.6$  (6.0) MeV. The irradiation time for each scanning position was approximately 1 h.

### III. RESULTS AND DISCUSSION

Figure 5 shows energy spectra of  $\gamma$  rays emitted from the target materials. The NRF peaks of  $^{206}\text{Pb}$  are observed at 5733, 5847, 5858, and 5904 keV in Fig. 5(a) obtained by irradiating the iron-concealed  $^{206}\text{Pb}$  cylinder. Those of  $^{208}\text{Pb}$  are also visible at 5292 and 5512 keV in Fig. 5(b) obtained by irradiating the natural lead blocks concealed in the iron box. Since the resonant energies of  $^{206}\text{Pb}$  are higher than the LCS  $\gamma$ -ray energy ( $E_\gamma^{\text{max}} = 5.6$  MeV), no NRF signal attributed to  $^{206}\text{Pb}$  is seen in Fig. 5(b). Figure 5(c) shows the energy spectrum obtained by the irradiation at the position  $z = \pm 22$  mm where the incident photon beam penetrates only the iron material. No NRF signal of both  $^{206}\text{Pb}$  and  $^{208}\text{Pb}$  is therefore observed in Fig. 5(c).

The relative intensities of 5904-keV  $\gamma$  rays in  $^{206}\text{Pb}$  and 5512-keV  $\gamma$  rays in  $^{208}\text{Pb}$  are plotted as a function of the irradiation position ( $z$ -direction) in Fig. 6. The intensities are normalized to the incident photon flux as well as the ground state  $\gamma$ -ray decay width  $\Gamma_0$ . The values of  $\Gamma_0 = 3.48 \pm 0.44$ <sup>12</sup> and  $23.0 \pm 3.6$  eV<sup>8</sup> are used for the resonances at 5904 keV in  $^{206}\text{Pb}$  and at 5512 keV in  $^{208}\text{Pb}$ , respectively. Attenuations of the incident photons by the target materials were corrected

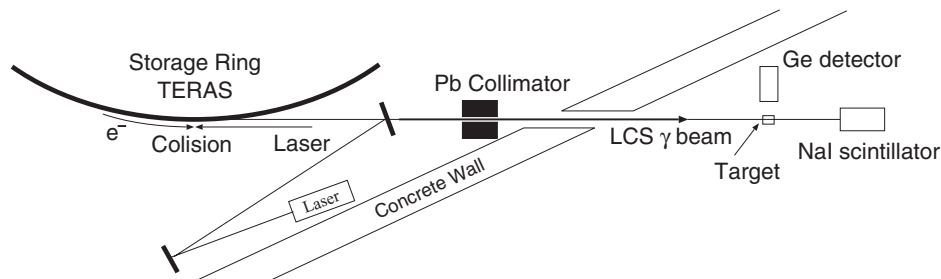


FIG. 2. Layout of the LCS photon beam line including the nuclear photon scattering measurement setup. NRF  $\gamma$  rays are detected by the HP-Ge detector. The NaI scintillator is used to monitor the flux of the incident  $\gamma$ -ray beam.

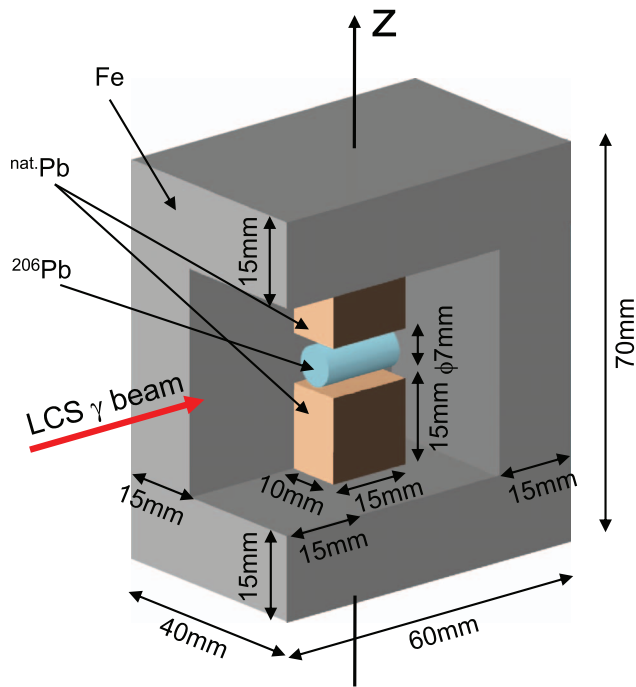


FIG. 4. (Color online) The interior of the target is shown. Natural lead ( $^{\text{nat}}\text{Pb}$ ) blocks and an enriched  $^{206}\text{Pb}$  cylinder are concealed in the iron box. The front and back side thickness of the iron box is 15 mm. The interrogation photon beam penetrates the iron shield. The target is moved vertically for scanning along the  $z$ -direction.

with the linear attenuation coefficients of photons taken from Ref. 13.

The relative intensities plotted in Fig. 6 are proportional to the effective thickness of the target material ( $^{206}\text{Pb}$  and  $^{208}\text{Pb}$ ) which is the product of the length, densities, and en-

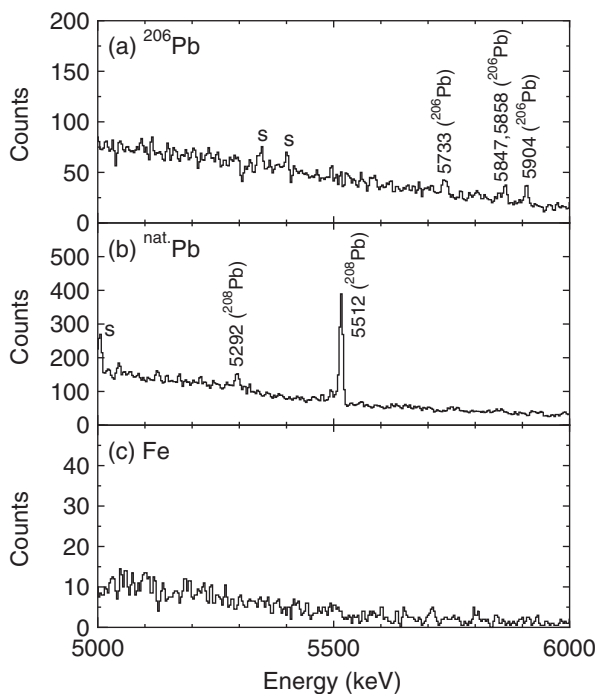


FIG. 5. NRF spectra obtained by the irradiation on the target materials. The irradiation positions are (a)  $-2 \leq z(\text{mm}) \leq 2$ , (b)  $-18 \leq z(\text{mm}) \leq -6$  and  $6 \leq z(\text{mm}) \leq 18$ , and (c)  $z = \pm 22$  mm. Peaks labels “s” are attributed to single escapes originated from the higher-energy NRF peaks.

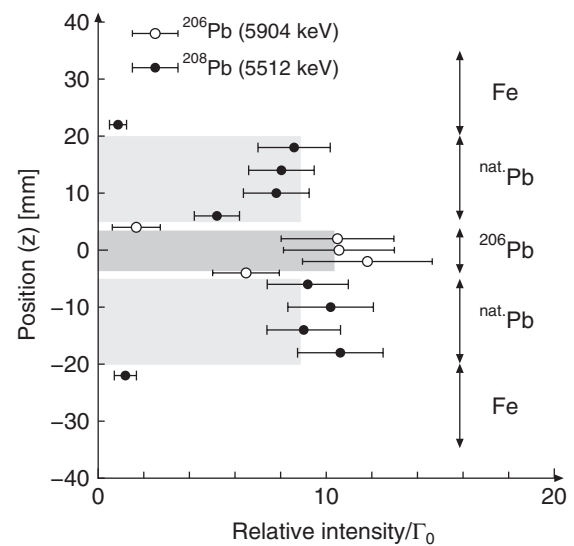


FIG. 6. Relative NRF intensities of the 5904 keV ( $^{206}\text{Pb}$ ) and 5512 keV ( $^{208}\text{Pb}$ )  $\gamma$  rays are plotted as a function of the irradiation position ( $z$ ). The intensities are normalized to the incident photon flux as well as the ground state decay width  $\Gamma_0$ . The error bars correspond to the statistical precision. The dark (light) gray box indicates the effective thickness of  $^{206}\text{Pb}$  ( $^{208}\text{Pb}$ ). The arrows show the width of the target materials.

richment/abundance of the targets. The measured ratio between the relative intensities of  $^{206}\text{Pb}$  and  $^{208}\text{Pb}$  is  $0.78 \pm 0.12$ . This is consistent with the value of 0.89, the ratio of effective thickness of  $^{206}\text{Pb}$  and  $^{208}\text{Pb}$ , within the quoted uncertainty. Thus, the isotopic concentration distribution can be obtained from the measured NRF spectra.

The detection limits of the present measurement setup are estimated to be 26 and 18 counts for the  $^{208}\text{Pb}$  and  $^{206}\text{Pb}$  cases, respectively, assuming the beam intensity of  $1.5 \times 10^5/\text{s}$  and the measurement time of 1 h which are the typical conditions of each measurement. Here, the detection limits are defined as  $3\sigma_b$ , where  $\sigma_b$  is the standard deviation of background counts. The smaller detection limit for  $^{206}\text{Pb}$  is possibly because of its smaller density of the target material ( $6.8 \text{ g/cm}^3$  for  $^{206}\text{Pb}$  and  $11.3 \text{ g/cm}^3$  for  $^{208}\text{Pb}$  with the same thickness of 15 mm), causing less background counts. The detection limit can be improved by increasing the counting statistics which is attainable by increasing the beam intensity and/or the measurement time. Under the above conditions, the detection limit is reduced to the effective thickness of  $1.6 (6.5) \text{ g/cm}^2$  for the  $^{208}\text{Pb}$  ( $^{206}\text{Pb}$ ) measurement setup. The larger value for  $^{206}\text{Pb}$  originates from the smaller ground state decay width.

The spatial resolution of the present isotope-specific NDA method depends on the size of the incident photon beam at the target position, determined by the collimator size. By using a 20-cm lead collimator with a small hole of 2-mm diameter placed 6 m downstream the collision point, the edge position can be extracted with 0.5 mm precision.<sup>14</sup> The present NRF method can be extended to two- to three-dimensional isotopic concentration mapping of isotopes of interest.<sup>15</sup> With a highly brilliant photon source which can be realized by the conjunction of technologies of laser supercavity and energy recovery linac accelerator,<sup>6</sup> precise isotope-specific mapping of clandestine materials can be performed.



#### IV. CONCLUSION

We have demonstrated the isotope-specific identification of lead materials concealed in a thick iron box based on the NRF method. A quasi-monochromatic photon beam generated by the inverse Compton scattering of laser light with high-energy electrons was used for resonant excitation of nuclear levels. We clearly observed 5904-keV  $\gamma$  ray in  $^{206}\text{Pb}$  and 5512-keV  $\gamma$  ray in  $^{208}\text{Pb}$  from the target materials concealed in a 15-mm thick iron box. The ratio of the effective thickness of the target materials can be deduced from the relative intensities of the NRF strength, enabling the isotope-specific quantification of the samples as well.

#### ACKNOWLEDGMENTS

This work was supported in part by the Grant-in-Aid for Scientific Research B (21360467) of the Ministry of Education, Culture, Sports, Science and Technology of Japan.

- <sup>1</sup>S. J. Tobin, N. P. Sandoval, M. L. Fensin, S. Y. Lee, B. A. Ludewigt, H. O. Menlove, B. J. Quiter, A. Rajasingum, M. A. Shear, L. E. Smith, M. T. Swinhoe, and S. J. Thompson, in *Institute of Nuclear Materials Management 50th Annual Meeting*, Tucson, AZ, 2009 (LA-UR 09-03748).
- <sup>2</sup>R. Hajima, N. Kikuzawa, N. Nishimori, T. Hayakawa, T. Shizuma, K. Kawase, M. Kando, E. Minehara, H. Toyokawa, and H. Ohgaki, *Nucl. Instrum. Methods Phys. Res. A* **608**, S57 (2009).

- <sup>3</sup>T. Hayakawa, N. Kikuzawa, R. Hajima, T. Shizuma, N. Nishimori, M. Fujiwara, and M. Seya, *Nucl. Instrum. Methods Phys. Res. A* **621**, 695 (2010).
- <sup>4</sup>W. Bertozzi and R. J. Ledoux, *Nucl. Instrum. Methods Phys. Res. B* **241**, 820 (2005).
- <sup>5</sup>J. Pruet, D. P. McNabb, C. A. Hagmann, F. V. Hartemann, and C. P. J. Barty, *J. Appl. Phys.* **99**, 123102 (2006).
- <sup>6</sup>R. Hajima, T. Hayakawa, N. Kikuzawa, and E. Minehara, *J. Nucl. Sci. Technol.* **45**, 441 (2008).
- <sup>7</sup>U. Kneissl, H. H. Pitz, and A. Zilges, *Prog. Part. Nucl. Phys.* **37**, 349 (1996).
- <sup>8</sup>T. Shizuma, T. Hayakawa, H. Ohgaki, H. Toyokawa, T. Komatsubara, N. Kikuzawa, A. Tamii, and H. Nakada, *Phys. Rev. C* **78**, 061303(R) (2008).
- <sup>9</sup>H. Ohgaki, H. Toyokawa, K. Kudo, N. Takeda, and T. Yamazaki, *Nucl. Instrum. Methods Phys. Res. A* **455**, 54 (2000).
- <sup>10</sup>W. R. Nelson, H. Hirayama, and W. O. Roger, *The EGS4 Code Systems*, SLAC-Report-**265** (1985).
- <sup>11</sup>T. Shizuma, H. Utsunomiya, P. Mohr, T. Hayakawa, S. Goko, A. Makinaga, H. Akimune, T. Yamagata, M. Ohta, H. Ohgaki, Y.-W. Lui, H. Toyokawa, A. Uritani, and S. Goriely, *Phys. Rev. C* **72**, 025808 (2005).
- <sup>12</sup>J. Enders, P. von Brentano, J. Eberth, A. Fitzler, C. Fransen, R.-D. Herzberg, H. Kaiser, L. Käubler, P. von Neumann-Cosel, N. Pietralla, V. Yu Ponomarev, A. Richter, R. Schwengner, I. Wiedenhöver, *Nucl. Phys. A* **724**, 243 (2003).
- <sup>13</sup>J. H. Hubbell, *Natl. Stand. Ref. Data Ser.* **29**, 62 (1969).
- <sup>14</sup>N. Kikuzawa, R. Hajima, N. Nishimori, E. Minehara, T. Hayakawa, T. Shizuma, H. Toyokawa, and H. Ohgaki, *Appl. Phys. Express* **2**, 036502 (2009).
- <sup>15</sup>H. Toyokawa, H. Ohgaki, T. Hayakawa, T. Kii, T. Shizuma, R. Hajima, N. Kikuzawa, K. Matsuda, F. Kitatani, and H. Harada, *Jpn. J. Appl. Phys.* **50**, 100209 (2011).